

## HOT WORKABILITY OF 95MnWCr5 TOOL STEEL

### VROČA PREOBLIKOVALNOST ORODNEGA JEKLA 95MnWCr5

Ažbe Križaj<sup>2</sup>, Matevž Fazarinc<sup>1</sup>, Monika Jenko<sup>2</sup>, Peter Fajfar<sup>1</sup>

<sup>1</sup>University of Ljubljana, Faculty of Natural Science and Technology, Aškerčeva cesta 12, SI-1000, Ljubljana, Slovenia

<sup>2</sup>Institute of Metals and Technology, Lepi pot 11, SI-1000 Ljubljana, Slovenia  
peter.fajfar@omm.ntf.uni-lj.si

*Prejem rokopisa – received: 2011-04-18; sprejem za objavo – accepted for publication: 2011-06-01*

The hot workability of a 95MnWCr5 medium-alloyed cold-work tool steel was investigated with hot-compression tests on a Gleeble 1500D thermo-mechanical simulator. The tests were performed in the temperature range 850–1150 °C and strain-rate range 0.001–10 s<sup>-1</sup>. With decreasing of the deformation temperature and increasing of the strain-rate values of the peak strain, the peak and steady-state stresses increase. The hyperbolic sine Arrhenius function was used to determine the apparent activation energy for the hot workability. The apparent activation energy of 356 kJ mol<sup>-1</sup> for entire hot-working range was calculated using the peak stresses. The power-dissipation maps exhibited a single domain with the peak of efficiency in the range 30–40 %, the temperature range 960–1100 °C and a strain rate of 1.0 s<sup>-1</sup>.

Key words: cold-work tool steel, hot workability, activation energy, power-dissipation maps

Raziskana je bila vroča preoblikovalnost orodnega jekla za delo v hladnem 95MnWCr5. Na termomehanskem simulatorju Gleeble 1500D so bili izvedeni tlačni preizkusi v temperaturnem območju 850–1150 °C in v območju hitrosti deformacije 0,001–10 s<sup>-1</sup>. S padajočo temperaturo deformacije naraščajo vrednosti najvišjih deformacij in napetosti ter napetosti pri stabilnem stanju. Z uporabo sinušiperbolične Arrheniusove funkcije je bila izračunana navidezna aktivacijska energija za vroče preoblikovanje. Na celotnem temperaturnem področju ter za maksimume napetosti tečenja izračunana aktivacijska energija je 365 kJ mol<sup>-1</sup>. Na mapah učinkovitosti porazdelitve energije je le eno območje z največjim izkoristkom v območju 30–40 %, in sicer pri temperaturah v območju 960–1000 °C in hitrosti deformacije 1,0 s<sup>-1</sup>.

Ključne besede: orodna jekla za delo v hladnem, vroča preoblikovalnost, aktivacijska energija, mapa učinkovitosti porazdelitve energije

## 1 INTRODUCTION

Tool steels are used for tools and dies where resistance to wear, toughness, strength at high temperatures and stability during heat treatment are required. These properties are achieved by a combination of solid-solution enrichment of the matrix (Mn, Si) and the effect of carbides (W, V, Cr). However, the presence of carbides makes the hot deformation very difficult.<sup>4,5</sup> The type of eutectic carbides, their quantity, morphology, size and distribution, depend on the chemical composition of the tool steel as well as on the production sequences route that lead to different initial microstructures and, consequently, to different hot-deformation abilities of the tool steels. Thus, a large number of parameters, i.e., chemical composition, processing parameters, deformation conditions, stress state, etc., which are usually mutually dependent, influences the hot workability of the tool steels that makes a study of the hot workability of these steels very demanding. It is now generally understood that the workability consists of two independent parts: the state-of-stress workability (SoS) and the intrinsic workability.<sup>1</sup> The SoS workability depends on the geometry of the deformation zone in which the workpiece is subject to a three-dimensional stress state. Thus, for obtaining good intrinsic workability, it is essential to select the appropriate process parameters to obtain the appropriate initial microstructure. The internal

behavior in the material during hot deformation, i.e., the hardening, dynamic recrystallization (DRX), etc., can be implicitly expressed by the shape and the height of the flow curves.<sup>2,3</sup>

The hot workability of tool steels and other steels has been studied by several authors.<sup>4–18</sup> Imbert *et al.*<sup>7–11</sup> investigated the hot workability of five different steel grades: A2, a medium carbon cold-work tool steel; D2, a high-carbon, high-chromium, cold-work die steel; M2, a high-speed steel; W1, a water-hardening, carbon tool steel; and H13, an air-hardening tool steel. For these grades that represent a wide variety of compositions (and carbide contents) continuous hot torsion tests were performed in the temperature range 900–1200 °C and strain rate range 0.1–4 s<sup>-1</sup>. In a series of continuous deformation tests, the flow stress and ductility were determined. The dependence of the static restoration on the pass strain, the strain rate, the temperature, and the time between passes were determined.<sup>2</sup> The influence of hard carbides particles and incipient melting on the intrinsic ductility as a function of temperature and strain rate for the A2, M2 and H13 tool steels was investigated.<sup>3</sup> The effect of temperature and strain rate on the DRX kinetics of the A2, M2, D2, W1 and K310 tool steels was analyzed. The dependence of the peak stress on the temperature and strain rate is represented very well by the hyperbolic sine Arrhenius function. The hot-deformation energies for the investigated tool steels were determined.

Večko Pirtovšek *et al.*<sup>4, 6, 13, 14</sup> used processing maps to investigate the hot workability of six different tool steel grades: A2, M2, D2, M42, 1.17 C–11.3 Cr–1.48 V–2.24 W–1.35 Mo and 1.2690 cold-work tool steel. Hot-compression tests were performed on a Gleeble 1500D thermo-mechanical simulator in the temperature range 850–1200 °C and strain-rate range 0.001–10 s<sup>-1</sup>. For increasing the hot workability of tool steels, several research steps were carried out, i.e., a determination of the appropriate casting temperature and cooling rate, soaking temperature, safe domain for hot working and chemical composition. The analysis carried out by the conditional average estimator neural network (CAE NN) revealed the influence of carbide-forming elements on the appearance of surface cracking during hot rolling. The results of the analysis were additionally supported by the THERMOCALC calculation.<sup>14</sup>

From the above-mentioned investigations it is clear that to avoid the unexpected occurrence of surface cracking during the hot deformation, due to the complexity of the hot workability of tool steels, for each type of tool steel the optimal hot-deformation conditions should be found. Namely, the safe domains for hot working for the studied tool steel are different, especially at the upper and lower limits of the safe domain for hot working.<sup>4</sup>

The 95MnWCr5 tool steel is one of the most widely used, general purpose, oil-hardening tool and die steels. Because of its high wear resistance and sufficient toughness, the 95MnWCr5 steel is used for a wide variety of tool and die applications, such as cutting and punching tools, shear knives, thread-rolling tools and measuring instruments. Furthermore, the constant pressure on the increase of its production as well as the demands on the hot rolling of the profiles with the lower final dimensions require reliable data through a wide range of hot-deformation conditions, i.e., data about its mechanical response during the hot deformation as well as about its deformation ability. In the literature, no reliable data about the hot working of 95MnWCr5 tool steel can be found. In the present work, the hot workability of the 95MnWCr5 medium-alloyed tool steel by hot-compression tests was investigated. Optimal deformation parameters of the hot working as well as constants for the hyperbolic sine Arrhenius equation were obtained. The efficiency of the power-dissipation map was used to reveal the appropriate range for the working conditions.

## 2 EXPERIMENTAL

The chemical composition of the 95MnWCr5 cold-work tool steel used in the present study is given in **Table 2**. The cylindrical specimens used for the compression tests were 10 mm in diameter and 15 mm in height and were machined from an annealed forged billet. The initial microstructure of the investigated steel is shown in **Figure 1**. The hot-compression tests were performed on a Gleeble 1500D thermal-mechanical

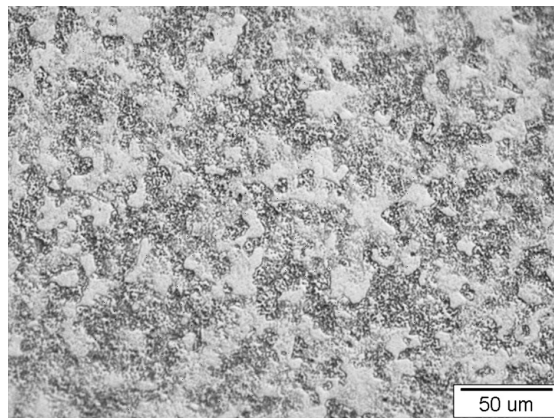


**Figure 1:** Initial microstructure of the specimen

**Slika 1:** Mikrostruktura osnovnega stanja

simulator in the temperature range 850–1150 °C and strain rates of 0.001–10 s<sup>-1</sup>. A time course of the temperature during the hot-compression test is shown in **Figure 2**. The specimens were heated with a rate of 3 °C s<sup>-1</sup> (1) to a soaking temperature of 1200 °C, held there for 10 min (2), and then cooled with a rate of 2 °C s<sup>-1</sup> to the deformation temperature (3), held for 10 min at the deformation temperature (4), deformed with a prescribed strain rate (5), and water quenched (6) to retain the recrystallized microstructures. For the reduction of the friction and to prevent mutual welding between the specimens and the tool anvil, a Ni-based lubricant, carbon and tantalum foils were used. The temperature of the test specimens was measured by means of an S-type thermocouple welded at the centre of the specimen's surface.

The specimens were sectioned along the compression axis and prepared for optical microscopy. The ferric chloride acid solution (5 g FeCl<sub>3</sub>, 10 g HCl in 100 mL Ethanol) was used for the etching. The microstructures in the centre of the section plane were examined using a NIKON MICROPHOT-FXA optical microscope with a HITACHI HV-C20A video camera, and Soft Imaging-

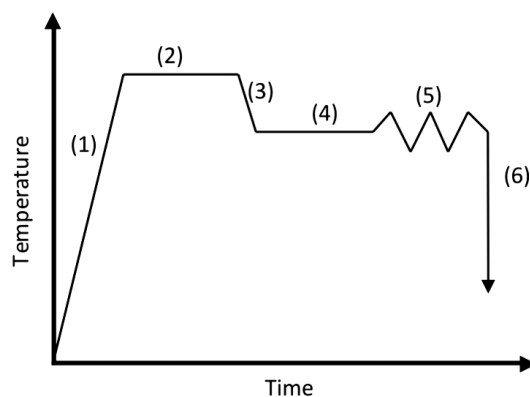


**Figure 2:** Time course of temperature during compression tests

**Slika 2:** Shematski prikaz poteka temperature vzorcev pri preizkusu vročega stiskanja

System analysis software for the metallographic image analysis.

### 3 RESULTS AND DISCUSSION

#### 3.1 Flow curves

Representative flow curves of the 95MnWCr5 cold-work tool steel obtained from a hot-compression test are shown in **Figure 3**. The flow curves exhibit the behavior of materials that undergo dynamic recrystallization (DRX) with strain hardening to the peak stress  $\sigma_p$  and later softening towards the steady-state stress  $\sigma_{ss}$ . The onset of the  $\sigma_p$  is less obvious at the higher strain rates (**Figure 3a**). The value of the peak strains for the strain rate of  $0.001 \text{ s}^{-1}$  is 0.14 and it increases up to 0.5 at the strain rate of  $10 \text{ s}^{-1}$ . The curves in the temperature range of 1200–1050 °C (**Figure 3b**) exhibit peaks and softening to a steady state, which indicates DRX behavior.

With decreasing the deformation temperature and increasing the strain rate, the values of the peak strain, peak and steady-state stress increase.

Activation energy for hot working

The activation energy of the deformation  $Q$  can be estimated using the following hyperbolic sine function:<sup>7,10,19,24</sup>

$$\dot{\epsilon} = A[\sinh(\alpha\sigma)]^n \exp\left(-\frac{Q}{RT}\right) \quad (1)$$

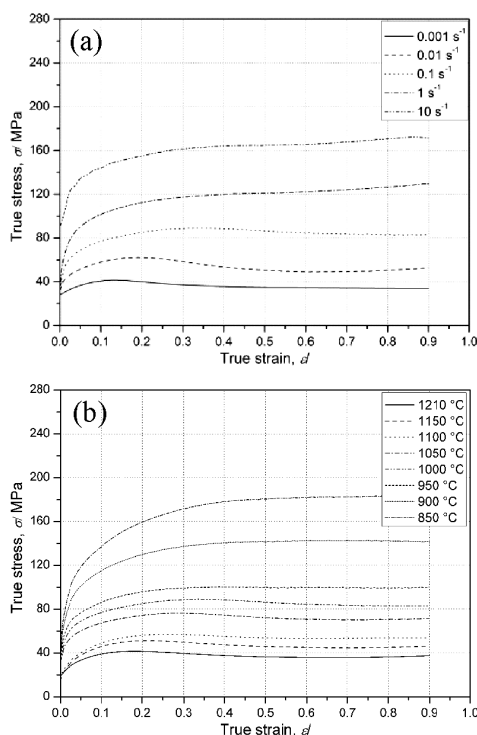


**Figure 3:** True stress / true strain curves for 95MnWCr5 a) at a temperature of 1000 °C, b) at a strain rate of  $0.1 \text{ s}^{-1}$

**Slika 3:** Krivulja tečenja jekla 95MnWCr5: a) pri temperaturi 1000 °C, b) pri hitrosti deformacije  $0.1 \text{ s}^{-1}$

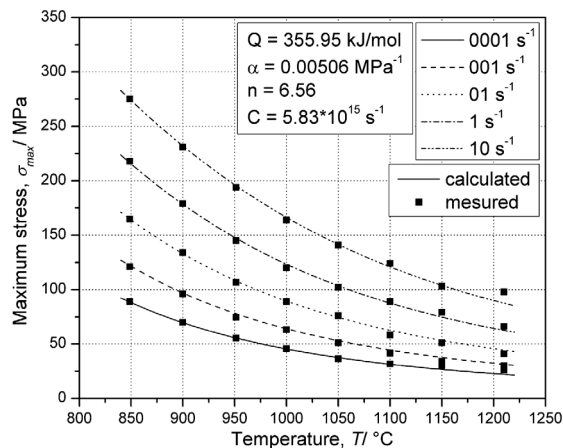


**Figure 4:** Comparison between the calculated and the measured peak stresses as a function of temperature and strain rate

**Slika 4:** Primerjava med izmerjeno in izračunano maksimalno napetostjo pri različnih temperaturah in hitrostih deformacije

where  $A$  and  $\alpha$  are material constants,  $n$  is the stress exponent,  $\dot{\epsilon}$  is the strain rate,  $\sigma$  is the flow stress,  $T$  is the absolute temperature and  $R$  is the universal gas constant. The method for calculating the parameters of Eq. 1 is described by Kugler.<sup>19</sup> The peak stresses of the flow curves were used for the calculation of the activation energy of the deformation and other constants. The comparison between the measured and calculated dependences of the peak stresses on the temperature for different strain rates is shown in **Figure 4**. A very good

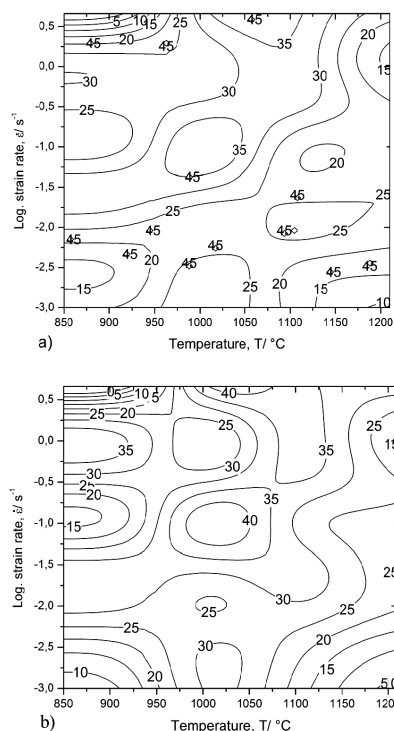


**Figure 5:** Efficiency of power-dissipation maps for 95MnWCr5 at different strains: a)  $\epsilon = 0.3$ , b)  $\epsilon = 0.9$

**Slika 5:** Učinkovitost porazdelitve energije za jeklo 95MnWCr5 pri različnih stopnjah deformacije: a)  $\epsilon = 0,3$ , b)  $\epsilon = 0,9$

fit of the data was obtained by taking  $\alpha = 0.005 \text{ MPa}^{-1}$  and  $n = 6.5$ . The value of the apparent activation energy of the deformation was  $356 \text{ kJ mol}^{-1}$ . This value for the activation energy was compared with other investigations, as summarized in **Table 1**. By comparing the results of the activation energies (**Table 1**) with the chemical composition of compared tool steels (**Table 2**), we can conclude that the obtained value of the activation energy is close to those for the A2 tool steel. Usually, this increases with the alloy contents and with the carbide volume fraction.<sup>10,12,23</sup> The activation energy for relatively pure iron is about  $280 \text{ kJ/mol}$ , and for low-carbon steel it is approximately  $300 \text{ kJ mol}^{-1}$ .<sup>24</sup>

**Table 1:** Values of the activation energy for the deformation of tool steels.

**Tabela 1:** Vrednosti aktivacijske energije za deformaciju orodnih jekel

Tool steel	$Q/(\text{kJ mol}^{-1})$	References
M2	455	C. A. C. Imbert <sup>12</sup>
D2	428	C. A. C. Imbert <sup>5</sup>
A2	399	C. A. C. Imbert <sup>12</sup>
A2*	400	T. Vecko Pirtovsek <sup>6</sup>
W1	286	C. A. C. Imbert <sup>5</sup>
K310	227	H. R. Ezatpour <sup>7</sup>
1.17C–11.3Cr–1.48V– 2.24W–1.35Mo	554	T. Vecko Pirtovsek <sup>4</sup>
M35	607	P. Fajfar <sup>5</sup>
95MnWCr5	356	Current work

### 3.2 Efficiency of the power-dissipation map and the microstructure of deformed specimens

The efficiency of power-dissipation maps was developed for the optimization of the hot-deformation process of materials. They represent an explicit response of a material, in terms of microstructural mechanisms, to the imposed process parameters.<sup>1,22</sup> The basis for power-dissipation maps is the Dynamic Materials Model (DMM), where a deformed workpiece is considered to be a dissipater of the power.<sup>23</sup> The characteristics of the power dissipation through microstructural changes are expressed in terms of the efficiency of the power dissipation,  $\eta$ :

**Table 2:** Chemical composition of tool steels in mass fractions, w/%

**Tabela 2:** Kemijska sestava orodnih jekel v masnih deležih, w/%

	C	Cr	Ni	Si	Mn	Mo	V	W	Co
M2	0,84	4,00		0,30	0,25	5,00	1,90		
D2	1,45	11,09	0,21	0,24	0,38	0,72	0,71		
A2	1,00	5,00		0,30	0,70	1,15	0,30		
A2*	0,99	4,95	0,15	0,28	0,48	0,94	0,18	0,08	
W1	1,03	0,07	0,14	0,23	0,31	0,03			
K310	0,83	1,9		0,45	0,40	0,30			
1.17C–11.3Cr–1.48V–2.2 4W–1.35Mo	1,17	11,3		0,24	0,26	1,35	1,48	2,24	
M35	0,91	4,15				4,7	2,1	6,3	4,75
95MnWCr5	0,95	0,48		0,25	1,20	0,94	0,13	0,55	

$$\eta = \frac{2m}{m+1} \quad (2)$$

$$m = \frac{\partial(\ln \sigma)}{\partial(\ln \dot{\epsilon})} \quad (3)$$

where  $m$  is the strain-rate sensitivity of the flow stress,  $\sigma$  is the flow stress and  $\dot{\epsilon}$  is the strain rate.

To obtain the optimal hot-working parameters of the investigated material, several maps for different strains must be calculated.<sup>1,13–15,22,23</sup> In the current work, the efficiency of the power-dissipation maps is presented in the temperature-strain rate plane for strains of 0.3 (**Figure 5a**) and (**Figure 5b**). The contour numbers represent the efficiency of the power dissipation  $\eta/\%$ . The domain of dynamic recrystallization at a strain of 0.3 is in the temperature range  $950\text{--}1020 \text{ }^\circ\text{C}$  and strain-rate range  $0.01\text{--}1 \text{ s}^{-1}$  with a maximum efficiency of 45 % at  $1005 \text{ }^\circ\text{C}$  and  $0.1 \text{ s}^{-1}$  (**Figure 5a**). The domain of dynamic recrystallization at a strain of 0.9 is in the temperature range  $970\text{--}1120 \text{ }^\circ\text{C}$  and strain-rate range  $0.01\text{--}1 \text{ s}^{-1}$  with a maximum efficiency of 40 % occurring at  $1005 \text{ }^\circ\text{C}$  and  $0.1 \text{ s}^{-1}$  (**Figure 5b**).

Carbide precipitates of vanadium, tungsten and chromium along austenite grain boundaries influence the ductility of the steel grade 95MnWCr5. The microstructure for the optimal range for hot working where DRX occurs (i.e.,  $1000 \text{ }^\circ\text{C}$ ,  $0.1 \text{ s}^{-1}$ ) is presented in **Figure 6a**. Deformation at higher temperatures (i.e.,  $1200 \text{ }^\circ\text{C}$ ) and the strain-rate range  $0.001\text{--}10 \text{ s}^{-1}$  causes cracks due to incipient melting at the grain boundaries (**Figure 6b**). At lower temperatures (i.e.,  $850 \text{ }^\circ\text{C}$ ) and higher strain rates (i.e.,  $10 \text{ s}^{-1}$ ), high stress values are responsible for void formation at the carbides, which leads to crack formation (**Figure 6c**). Material flow instability also occurs at strain rate of  $1 \text{ s}^{-1}$  in the form of twinning (**Figure 6d**).

Thus, all the areas with too high or too low values of efficiency of power dissipation should be avoided during hot deformation, if possible. On the other hand, hot deformation in areas with values in the range 30–40 % should be intensified.

As mentioned in the introduction, the hot deformability of each of the individual tool steels is not a

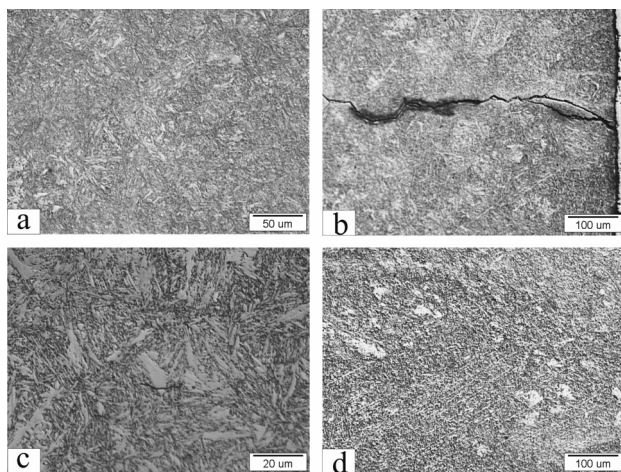


**Figure 6:** Microstructure of 95MnWCr5: a)  $T = 1000\text{ }^{\circ}\text{C}$ ,  $\dot{\epsilon} = 0.1$ , b)  $T = 1200\text{ }^{\circ}\text{C}$ ,  $\dot{\epsilon} = 1.0$ , c)  $T = 1150\text{ }^{\circ}\text{C}$ ,  $\dot{\epsilon} = 10.0$ , d)  $T = 850\text{ }^{\circ}\text{C}$ ,  $\dot{\epsilon} = 1.0$ ,  
**Slika 6:** Mikrostruktura jekla 95MnWCr5: a)  $T = 1000\text{ }^{\circ}\text{C}$ ,  $\dot{\epsilon} = 0.1$ , b)  $T = 1200\text{ }^{\circ}\text{C}$ ,  $\dot{\epsilon} = 1.0$ , c)  $T = 1150\text{ }^{\circ}\text{C}$ ,  $\dot{\epsilon} = 10.0$ , d)  $T = 850\text{ }^{\circ}\text{C}$ ,  $\dot{\epsilon} = 1.0$

constant value. A variation in the processing parameters as well as in the chemical composition can lead to widening/narrowing of the safe/unsafe domain for hot working.

#### 4 CONCLUSION

The hot workability of 95MnWCr5 cold-work tool steel was investigated by means of hot-compression tests. The tests were conducted in the temperature range 850–1150 °C in intervals of 50 °C and in the strain rate range 0.001–10 s<sup>-1</sup>. A Gleeble 1500D thermo-mechanical simulator was applied. The following conclusions can be drawn from this investigation:

The flow curves exhibit the behavior of materials that undergo dynamic recrystallization DRX with strain hardening to the peak stress  $\sigma_p$  and then work softening towards a steady-state stress  $\sigma_{ss}$ . The onset of  $\sigma_p$  is less obvious at higher strain rates and lower temperatures.

The apparent activation energy  $Q$  for hot deformation has a value of 356 kJ mol<sup>-1</sup>, and the stress exponent has a value of 6.5.

The optimum domain for hot working is in the temperature range 960–1050 °C, and a strain rate of 1.0 s<sup>-1</sup> with a peak efficiency of power dissipation  $\eta$  of about 30–40 % was found.

The domain of dynamic recrystallization at a strain of 0.9 is in the temperature range 970–1120 °C and strain rate range 0.01–1 s<sup>-1</sup> with a maximum efficiency of 40 % occurring at 1005 °C and 0.1 s<sup>-1</sup>.

The material exhibits flow instability at temperatures of 850 °C and 1200 °C for the entire range of the strain rate, and at the strain rate of 10 s<sup>-1</sup> for the entire range of temperatures.

#### 5 REFERENCES

- <sup>1</sup> Y. V. R. K. Prasad, S. Sasidhara, Hot Working Guide: A Compendium of Processing Maps, ASM International, Materials Park, OH, (1977), 543
- <sup>2</sup> G. Kugler, R. Turk, Acta Materialia, 52 (2004), 4659–4668
- <sup>3</sup> T. Vecko - Pirtovsek, I. Perus, G. Kugler and M. Terčelj, ISIJ International, 49 (2009) 3, 395–401
- <sup>4</sup> T. Večko - Pirtovšek, G. Kugler, M. Godec, M. Terčelj, Materials Characterization, 62 (2011), 189–197
- <sup>5</sup> P. Fajfar, D. Bombač, B. Markoli, RMZ – Materials and Geoenvironment, 57 (2010) 2, 159–164
- <sup>6</sup> T. Večko - Pirtovšek, I. Peruš, G. Kugler, R. Turk, M. Terčelj, Metalurgija, 47 (2008) 4, 307–311
- <sup>7</sup> C. Imbert, N. D. Ryan, H. J. McQueen, Metallurgical Transaction A, 15A (1984), 1855–1864
- <sup>8</sup> C. A. C. Imbert, H. J. McQueen, Canadian Metallurgical Quarterly, 40 (2001), 235–244
- <sup>9</sup> C. A. C. Imbert, H. J. McQueen, Materials Science and Engineering A, 313 (2001), 104–116
- <sup>10</sup> C. A. C. Imbert, H. J. McQueen, Materials Science and Technology, 16 (2000), 524–531
- <sup>11</sup> C. A. C. Imbert, H. J. McQueen, Materials Science and Engineering A, 313 (2001), 88–103
- <sup>12</sup> H. R. Ezatpour, S. A. Sajjadi, M. Haddad Sabzevar, Materials Science and Engineering A, 527 (2010), 1299–1305
- <sup>13</sup> T. Večko - Pirtovšek, G. Kugler, M. Godec, R. Turk, M. Terčelj, RMZ – Materials and Geoenvironment, 53 (2006), 1, 93–101
- <sup>14</sup> T. Večko - Pirtovšek, M. Fazarinc, G. Kugler, M. Terčelj, RMZ – Materials and Geoenvironment, 55 (2008), 2, 147–162
- <sup>15</sup> G. Roberts, G. Krauss, R. Kennedy, Tool Steels, ASM International, (1998), 364
- <sup>16</sup> F. Tehovnik, B. Arzenšek, B. Arh, Metalurgija, 47 (2008) 2, 75–79
- <sup>17</sup> F. Tehovnik, F. Vodopivec, R. Celin, B. Arzenšek, J. Gontarev, Mater. sci tehnol., 27 (2011) 4, 774–782
- <sup>18</sup> A. Kveder, Železarski zbornik 10 (1976) 4, 179–192
- <sup>19</sup> G. Kugler, M. Knap, H. Palkowski, R. Turk, Metalurgija, 43 (2004) 4, 267–272
- <sup>20</sup> C. A. C. Imbert, H. J. McQueen, Materials Science and Engineering A, 313 (2001), 88–103
- <sup>21</sup> P. V. Sivaprasad *et al*, Journal of Materials Processing Technology, 132 (2003), 262–268
- <sup>22</sup> Y. V. R. K. Prasad, H. L. Giegel, S. M. Doraivelu, J. C. Malas, J. T. Morgan, K. A. Lark, D. R. Baker, Metallurgical Transaction A, 15A (1984), 1883–1883
- <sup>23</sup> M. M. Myshlyayev, H. J. McQueen, A. Mwembela, E. Konoplev, Materials Science and Engineering A, 337 (2002), 121–133
- <sup>24</sup> H. J. McQueen, S. Yue, N. D. Ryan, E. Fry, Journal of Materials Processing Technology, 53 (1995), 293–310